IJPAC
© Global Research Publications

Vol. 10 • No. 1 • January-March 2015
pp. 1-8

Green Synthesis of Stable CdS Nanoparticles from Imidazolium Ionic Liquids and their Antibacterial Activities

K. Rajathi[1] and A. Rajendran[2*]

[1]Research and Development Centre, Bharathiar University, Coimbatore, Tamil Nadu, India
[2]Department of Chemistry, Sri Theagaraya College, Chennai, Tamil Nadu, India

ABSTRACT: Green synthesis of nanoparticles has paved way for better methodologies and newer approaches in the field of medicine. The present paper explores the synthesis of stable CdS nanoparticles using imidazolium based ionic liquids [BMIM] BF_4, [BMIM] PF_6, [BEMIM] BF_4, [BEMIM] PF_6 as green catalysts. Size controlled CdS nanostructures with distinct morphologies have been successfully synthesized and this process was found to be simple, fast, feasible and ecofriendly. The characterization of the nanoparticles such as their size and shape was performed by X-ray Diffraction (XRD) and Scanning Electron Microscope (SEM) techniques. Pure Ionic liquids and the as synthesized CdS nanoparticles were screened for their antibacterial activities. From the results, it appeared that the all tested imidazolium ionic liquids stabilized CdS nanoparticles are the less effective products against the tested bacterial strains compared with the anti- microbial activity of pure ionic liquids except Pure [BMIM] PF_6.

Keywords: Ionic liquids, CdS nanoparticles, Scanning Electron Microscope, X-ray Diffraction, Antimicrobial Activities.

INTRODUCTION

Ionic liquids (ILs) have shown tremendous promise as replacements for volatile organic solvents. ILs have been widely studied as a new kind of reaction media for the synthesis of nanoparticles owing to their unique properties such as extremely low volatility, wide liquid temperature range, good thermal stability, designable structure, high ionic conductivity, air and water stability, low toxicity, non-flammability, wide electro thermal window, etc. [1,2]. One of the most important environmental applications of nanomaterials is their use as sensors with enhanced monitoring capabilities for pollutants. They are used for treating contaminated water, soil or air and in green technologies to eliminate or reduce harmful emissions and wastes from industry using photocatalytic processes [3–5]. Semiconductor nanoparticles have optical and electrical properties that vary as a function of the particle size. The variability of these properties allows nanoparticles to be tailored for specific applications, such as II–VI semiconductors nanoparticles attract more attention because of their easy synthesis in the required size range. CdS is one of the very important II–VI direct band gap semiconductors; among the II–VI semiconductor compounds, CdS is a promising material because of their applications in optoelectronics [6], photo catalysts [7], solar cell [8] and nonlinear optical material [9]. Especially, they have been extensively exploited as materials to be used in biological systems, living organisms and drugs [10]. The present work focuses the synthesis of stable CdS nanoparticles using the imidazolium ILs such as liquids [BMIM] BF_4, [BMIM] PF_6, [BEMIM] BF_4 and [BEMIM] PF_6. The as synthesized CdS nanoparticles were screened for their antibacterial activities against gram (-) and gram (+) bacteria such as *Staphylococcus aureus* (Sa); *Micrococcus luteus* (MI); *Bacillus cereus* (Bc); *Escherichia coli* (Ec); *Pseudomonas aeruginosa* (Pa) and *Aeromonas hydrophila* (Ah).

EXPERIMENTAL

Materials

All chemicals such as 1-methyl imidazole, 1-bromobutane, Bromoethane, NaH, Acetonitrile,

* *To whom correspondence be made:*
E-mail: annamalai_rajendran2000@yahoo.com

Ether and Trichloroethane, ethyl acetate, Sodium tetraflouroborate ($NaBF_4$), Dichloroethane, Potassium hexafluorophosphate, Magnesium sulfate, Ammonium tetraflouroborate (NH_4BF_4), Cadmium acetate dihydrate, Thioacetamide (TAA), and Ethanol were of AR grade. They were purchased from Merk, SD Fine Chemicals Limited and used without further purification. All the solvents and reagents were used as received and all reactions were run in oven-dried glassware. The homogeneity of the products was checked on TLC plates coated with silica gel-G and visualized by exposure to iodine vapors. Double distilled water was used for synthesis and antibacterial studies.

Synthesis of Cadmium sulphide Nanoparticles

1-butyl-3-methylimidazolium tetrafluoroborate [BMIM] BF_4, 1-butyl-3-methylimidazolium hexafluorophosphate [BMIM] PF_6, 1-butyl-2-ethyl-3-methylimidazolium tetrafluoroborate [BEMIM] BF_4, 1-butyl-2-ethyl-3-methylimidazolium hexafluoro phosphate [BEMIM] PF_6 were prepared according to the literature [11]. In a typical synthesis procedure, cadmium acetate dihydrate (5.06 g) was dissolved in 12.5 ml of distilled water, and 12.5 ml of the ionic liquid under stirring at room temperature. In addition, 1.50 g of thioacetamide (TAA) was dissolved in 12.5 ml of distilled water, and 12.5 ml of the ionic liquid. Then, the TAA solution was slowly added into the solution of cadmium acetate under magnetic stirring [12]. The solution was refluxed approximately at 95°C for 60 min. The formed yellow color suspension was centrifuged to get the precipitate which was then washed three times with double distilled water and ethanol, respectively to remove the unreacted reagents and dried in an oven at 50°C for 24 h.

Characterization

The ^{1}H-NMR and ^{13}C-NMR spectra were recorded in $CDCl_3$ and DMSO-d_6 on a Joel JNN ECX 400P spectrometer. The FT–IR spectra were obtained on a Varian 800 FT-IR as thin films or for solid samples. The phase, purity and crystalline size of the CdS nanoparticles were characterized by powder X-ray diffraction (powder XRD) and Scanning Electron Microscope (SEM). The X-ray diffraction (XRD) patterns were recorded on a Philips Xpert X-ray diffractometer with Cu Kα radiation (λ = 0.15406 nm) employing a scan rate of 1° / min in the 2θ range from 20° to 80°. Surface morphology and the distribution of particles were characterized by a LEO 1430VP scanning electron microscopy (SEM) using an accelerating voltage of 15 kV. The XRD data were used to estimate the size of the constituent crystallites by Scherer's equation. The average particle size, D was determined by Eq. $D = K\lambda / (\beta.Cos\theta)$. Where λ is the wavelength of X-ray radiation (0.15406), K the Scherer's constant (K = 0.9), θ the characteristic X-ray radiation and β is full width at half maximum of the plane. The samples used for SEM and EDX observations were prepared by transferring the particles, which were first dispersed in ethanol, to a glass substrate attached to the SEM stage. After the evaporation of ethanol from the substrate, the particles on the stage were coated with a thin layer of gold and palladium.

Antimicrobial Activity (Broth dilution assay)

Antimicrobial activity of the as synthesized CdS nanoparticles was carried out using Broth dilution technique. In this method, a series of fifteen test tubes were filled with 0.5 ml sterilized nutrient broth. Sequentially, test tubes 2–14 received an additional 0.5 ml of the sample serially diluted to create a concentration sequence from 500 – 0.06 µg. The first test tube served as the control [13]. All the test tubes received 0.5 ml of inoculums. The test tubes were vortexed well and incubated for 24 h at 37 °C. The resulting turbidity was observed, and after 24 h, the minimum inhibition concentration (MIC) was determined where growth was no longer visible by assessment of turbidity by optical density readings at 600 nm.

RESULTS AND DISCUSSION

FT- IR Spectra

FT-IR spectra of pure [BMIM] BF_4 and CdS nanoparticles in [BMIM] BF_4, pure [BMIM] PF_6 and CdS nanoparticles in [BMIM] PF_6, pure [BEMIM] BF_4 and CdS nanoparticles in [BEMIM] BF_4 and pure [BEMIM] PF_6 and CdS nanoparticles in [BEMIM] PF_6 ionic liquid solutions are presented in figures 1-a,1-b,1-c and 1-d respectively and the main frequencies of peaks are listed in table1. Compared with the pure ionic liquids, several significant changes are observed in the FT-IR spectra of the CdS nanoparticles in ionic liquid solutions. The above changes of bands demonstrate that CdS nanoparticles have an effect on the electron cloud density of imidazole ring.

Table 1
Frequencies of FT-IR absorption bands for the Pure ILs-1, 2 and the ILs in CdS

[BMIM]BF_4 (IL-1), cm^{-1}	*IL-1 in CdS, cm^{-1}*	*[BMIM]PF_6 (IL-2) cm^{-1}*	*CdS in IL-2 (2a) cm^{-1}*	*[BEMIM]BF_4 (IL3) cm^{-1}*	*CdS in IL-3(3a) cm^{-1}*	*[BEMIM]PF_6 (IL-4) cm^{-1}*	*CdS in IL-4(4a) cm^{-1}*	*Assignment*
3425,3160, 3117	3743, 3153, 3113	3660, 3402, 3399, 3170, 3124	3164, 3120	3407,3158	3429, 3124	3413,3165	3858, 3743, 3567	C-H of imidazole ring stretching vibration
2971,2964, 2875	2967, 2871	2974, 2967, 2877, 2455	2957, 2872	2966,2877, 2202	2956, 2870	2967,2877, 2203	2940	The stretching vibrations of the methyl and methylene groups
1633	1643	-	1696	1659	1641	1662	1645	C=C stretching vibration
1573,1520, 1463	1555, 1461	1574, 1520, 1464	1557, 1461	1580,1533, 1462	1520, 1456	1581,1533, 1461	1517, 1460	C-H of imidazole ring inplane deformation vibration
1383,1286, 1234,1168, 1054	1387,1166, 1056	1386,1340, 1288, 1235,1169	1384,1165, 1103	1389	1377,1236, 1068	1388,1238117 0,1118	1380,1129	stretching vibration of anions
Below 1000	Below 1000	Below 1000	Below 1000	Below 1000	Below 1000	Below 1000	Below 1000	m-substituted imidazole ring

1-[BMIM] BF_4; 1a – CdS of [BMIM] BF_4; 2 - [BMIM] PF_6; 2a – CdS of [BMIM] PF_6, 3- [BEMIM] BF_4; 3a – CdS of [BEMIM] BF_4; 4 - [BEMIM] PF_6; 4a – CdS of [BEMIM] PF_6

Based on the analysis of FT-IR spectra, it is concluded that there are strong interactions between RTILs and cadmium sulphide, and the interactions focus on the imidazole ring of RTILs. Present findings showed similarity to the results previously reported [14].

XRD Analysis

The phase, purity and crystallite size of the CdS nanoparticles were studied by XRD. The typical diffraction pattern shows that the CdS nanoparticles prepared with different ionic liquids are crystalline in nature, high purity and free of impurities. The XRD pattern of the as prepared CdS nanoparticle in [BMIM] BF_4 (figure 1a) shows a hexagonal crystal structure. The major strong characteristic peaks of CdS particles are obtained at 2θ = 26.60, 36.06, 43.60, 47.76, 51.53 and 70.8, which are corresponding to crystal faces (100), (102), (110), (103), (112) and (211) of CdS respectively. All the reflection peaks could be indexed to hexagonal, primitive, (JCPDS NO 41-1049). In addition to identification of the crystalline phases, XRD data were used to estimate size of the constituent crystallites by Scherrer equation [15]. The average particle size, D, was determined using $D = K\lambda/\beta \cos\theta$ Where, λ is the wavelength of X-ray radiation (0.15406), K, the Scherrer×s constant (K=0.9), θ the characteristic X-ray radiation (2θ = 44.30) and β is the full-width-half-maximum of the (220) plane (in radians). According to the full width at half maximum of the diffraction peaks, the average size of the particles could be estimated from the Scherer equation to be about 1.8 nm.

Figure 1b shows the powder XRD pattern of the CdS nanoparticle prepared by using [BMIM] PF_6. All the peaks appear in the X-ray diffraction pattern (111), (220), (311) and (331) are in correspondence with that of cubic, face centered cubic structure, CdS nanoparticle (JCPDS NO 89-0440). The average size of the particles was found to be 3.26 nm.

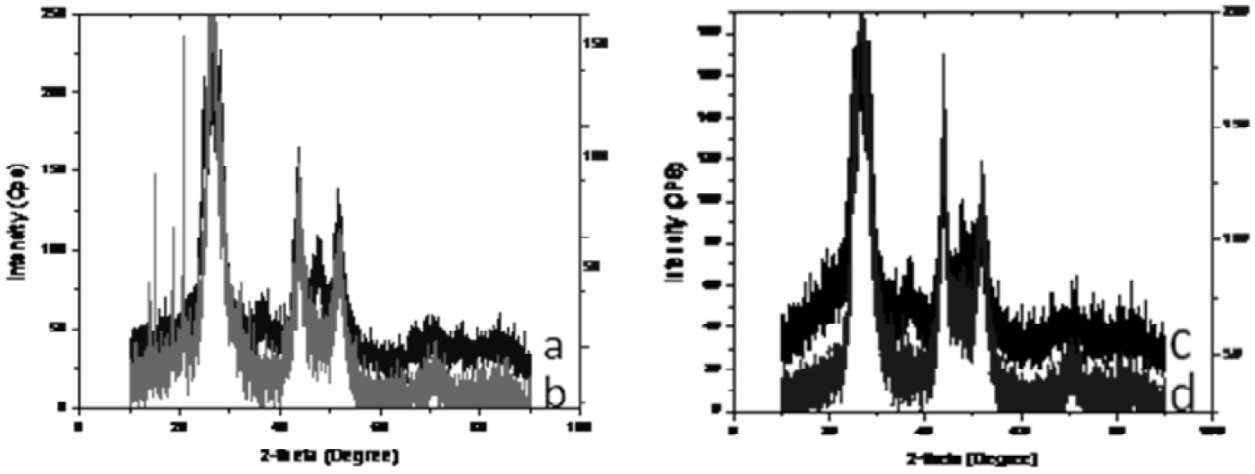

(a) CdS in [BMIM] BF_4; (b) CdS in [BMIM] PF_6 ; (c) CdS in [BEMIM] BF_4; (d) CdS in [BEMIM] PF_6

Figure 1: Powder XRD Pattern of as - prepared CdS nanoparticles in various ILs

Figure 1c shows the XRD pattern of synthesized CdS nanoparticles in [BEMIM] BF4. All the diffraction peaks can be identified to orthorhombic, primitive structure (a ≠ b ≠ c) of CdS nanoparticle (a ≠ b ≠ c). The values are matched to those in the JCPDS values (card No. 47-1179). The (313), (110) and (028) reflections of the primitive crystallites are clearly distinguished in the XRD pattern of the CdS nanocrystals. No peaks attributable to possible impurities are observed. It is apparent from the figure 1c that the products have the same orthorhombic, primitive structure and broadening in the patterns indicates that the CdS nanoparticles are very small in size. The mean particle sizes obtained for as prepared CdS nanoparticle is about 1.78 nm.

The powder XRD pattern of the product (CdS nanoparticle) prepared in [BEMIM] PF6 is displayed in figure 1d and the peaks are assigned to diffraction from the (002), (110), (112), and (211) planes of hexagonal, primitive (a = b ≠ c), (JCPDS

NO 41-1049) cadmium sulphide respectively [16,17]. According to the full width at half maximum of the diffraction peaks, the average size of the particles could be estimated from the Scherer equation to be about 2.04 nm.

SEM Analysis

Morphology of the as synthesized CdS nanoparticles in four different ILs was investigated by scanning electron microscope (SEM) recorded at different magnifications are shown in figures 3a-d. Figure 3a shows the SEM image of CdS nanoparticle prepared in [BMIM] BF_4. It is inferred that the structure of the nanoparticles is nanospheres with different sizes. It is quite apparent that aggregation of the nanoparticles has been controlled by ionic liquids. Morphologies of nanoparticles can also be

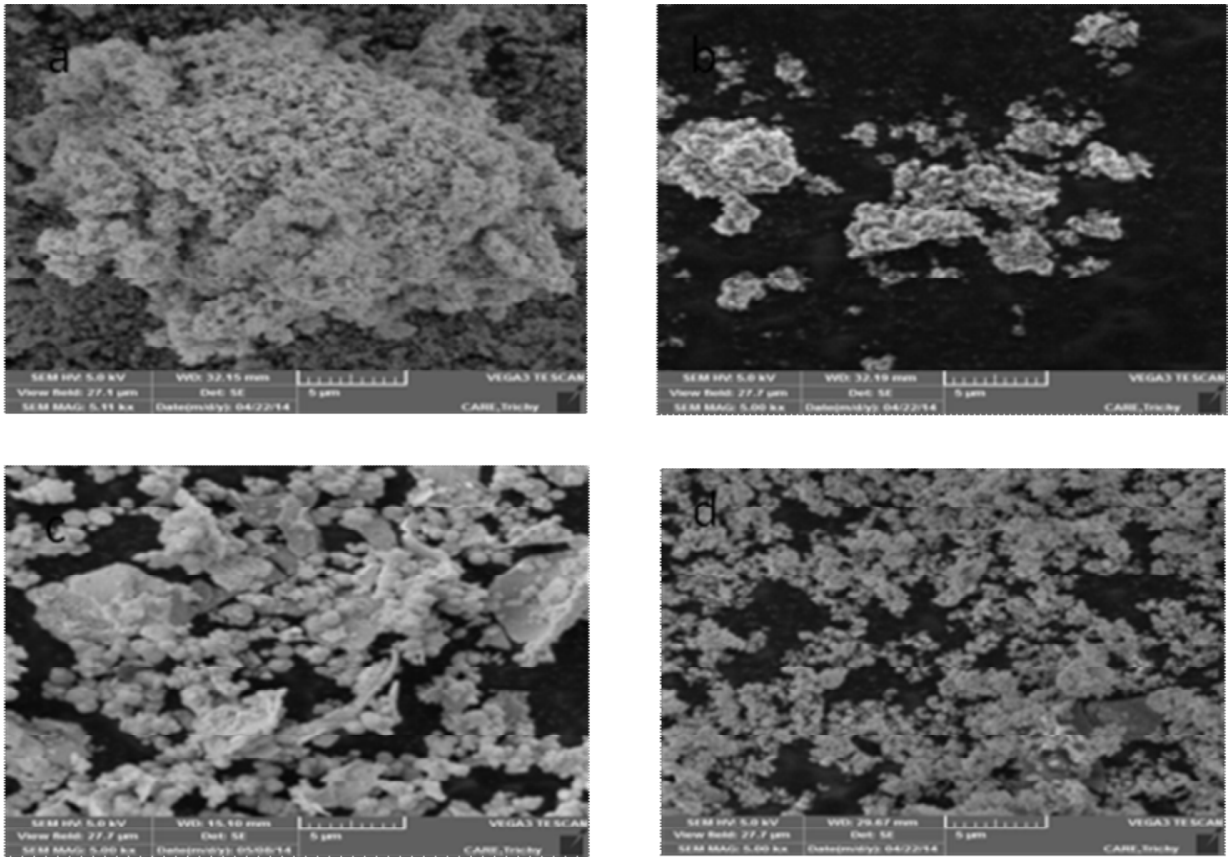

(a) CdS in [BMIM]BF_4; (b) CdS in [BMIM]PF_6 ; (c) CdS in [BEMIM]BF_4; (d) CdS in [BEMIM]PF_6 .

Figure 2: SEM images of as- prepared CdS nanoparticles

explained by the assistance of IL. The already formed CdS get coated by IL because of electrostatic phenomena between the cations of IL and nuclei of CdS.

The morphologies and dispersity of synthesized nanostuctured CdS samples from [BMIM] PF_6 is shown in Figure 3b. It can be seen from the SEM images that the morphology of CdS from [BMIM] PF_6 exhibit the well-defined CdS nanostructure composed of nanosized, regular and uniform spherical shaped particles with an average particle size of around 4 nm. Morphology of the CdS nanoparticles synthesized in [BEMIM] BF_4 is shown in figure 3c. It is evident that structure of the nanoparticles produced in neat IL, is small spherical in shape which is because of lower aggregation of nanoparticles.

Figure 3d shows the SEM image of CdS nanoparticle assisted by [BEMIM] PF_6. The morphology of CdS nanoparticles prepared in [BEMIM] PF_6, rather closely resembles that of CdS nanoparticles synthesized in previously discussed ILs. The reasons attributed for the observed morphology and dispersity of all CdS nanoparticles synthesized in all chosen ILs are also almost same. It is evident that structure of the nanoparticles

produced in water as solvent, is highly aggregated possessing irregular shapes and size of the particles is very high. In comparison, the samples prepared in presence of ILs have lower aggregation and size of aggregated nanoparticles, especially in neat IL, is small [12]. Therefore, IL as a solvent has an important and pivotal role in getting smaller nanoparticles. SEM analysis clearly indicates that the different characteristic ionic liquids produced the CdS particles with well-defined and extended ordered morphology without any agglomeration and aggregation.

EDX Analysis

The purity and composition of the products (CdS nanoparticle in [BMIM] BF_4, [BMIM] PF_6, [BEMIM] BF_4 and [BEMIM] PF_6 were studied by energy dispersive X-ray spectroscopy (EDX). The results are displayed in figure 4a-d. The other peaks in the figure corresponded to gold, palladium, and silicate which were due to sputter coating of the glass substrate on the EDX stage, and these were not considered in the elemental analysis of CdS. It is clear that the CdS nanoparticles prepared were sufficiently pure.

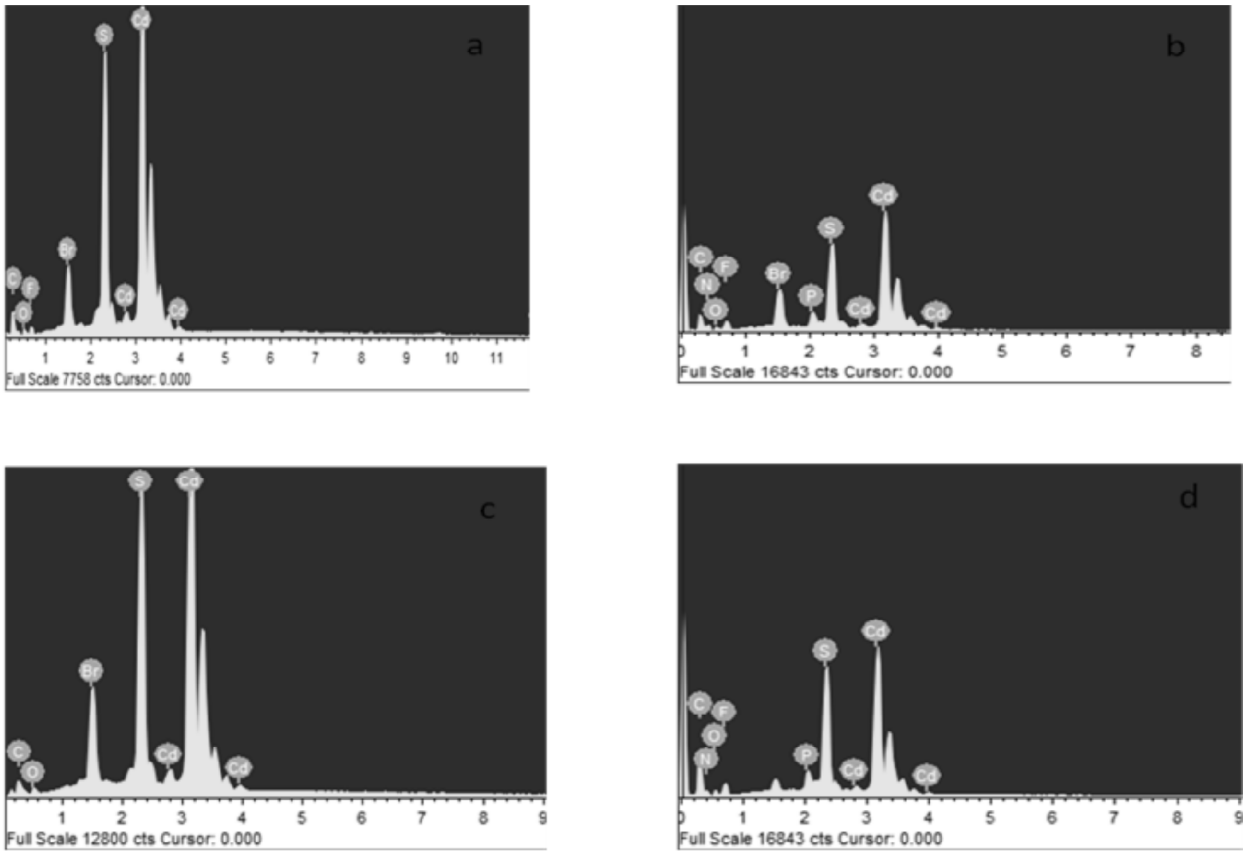

(a) CdS in [BMIM]BF_4; (b) CdS in [BMIM]PF_6 ; (c) CdS in [BEMIM]BF_4; (d) CdS in [BEMIM]PF_6.

Figure 3: EDX patterns of as- prepared CdS nanoparticles in various ILs

Antimicrobial Activities

The antibacterial activities of as synthesized CdS nanoparticles in four different ILs were screened with three gram positive (*Staphylococcus aureus*, *Micrococcus luteus* and *Bacillus cereus*) and three gram negative bacteria (*Escherichia coli*, *Pseudomonas aeruginosa* and *Aeromonas hydrophila*) using broth dilution technique. The results are presented in table 2. Gram negative MIC having thin simple multilayered lipid materials within the cell wall, the CdS nanoparticles simply enter into microorganism cells; thus, these show high inhibition zone than the opposite bacteria. CdS nanoparticles possess well-developed surface chemistry, chemical stability and applicable smaller size than a microorganism, which makes them easier to interact with the microorganisms.

Table 2
The MIC of CdS nanoparticles solution stabilized by ionic liquids

Compoundnumber	*Compound*	*MIC (μg/mL)*					
		Tested organisms (bacteria)					
		Sa	*Ml*	*Bc*	*Ec*	*Pa*	*Ah*
1	Pure [BMIM] BF_4	31.25	31.25	31.25	15.63	31.25	31.25
1a	CdS in [BMIM] BF_4	62.50	62.50	125.00	125.00	62.50	125.00
2	Pure [BMIM] PF_6	250	62.5	31.25	250	250	62.5
2a	CdS in [BMIM] PF_6	15.63	15.63	15.63	62.50	31.25	31.25
3	Pure [BEMIM] BF_4	15.63	31.25	15.63	15.63	31.25	62.5
3a	CdS in [BEMIM] BF_4	62.50	31.25	15.63	125.00	62.50	62.5
4	Pure [BEMIM] PF_6	0.98	15.63	15.63	0.98	0.98	7.81
4a	CdS in [BEMIM] PF_6	125.00	31.25	62.50	125.00	125.00	125.00

Sa- Staphylococcus aureus; Ml - Micrococcus luteus; Bc - Bacillus cereus; Ec - Escherichia coli; Pa - Pseudomonas aeruginosa and Ah - Aeromonas hydrophila

Nanoparticles are additionally able to maintain a constant form and size in solution. It would be that the particles interact with the building components of the outer membrane inflicting structural changes, degradation and at last, death. Also, fascinating results spurred out once the CdS nanoparticle concentration was increased. The microbe activity was increased higher as the nanoparticle concentration was increased. In view of the results, it appeared that the all tested imidazolium ionic liquids stabilized CdS nanoparticles are the less effective products against the tested bacterial strains compared with the anti- microbial activity of pure ionic liquids except Pure [BMIM] PF_6. The reason is that as CdS particle size is increased, additional quantity of antibiotics gets adsorbable on the nanoparticle surfaces and clearly this can increase the microorganism activity. Since the amount of antibiotics molecules increase, it'll act additional effectively against the microorganisms. From these observations, it is verified that CdS nanoparticles act as a decent anchor carrying additional quantity of antibiotics effectively on its surface via static attraction between the amine groups of antibiotics and nanoparticles thereby increasing the increased activity [18].

CONCLUSION

CdS nanoparticles were prepared in presence of [BMIM] BF_4, [BMIM] PF_6, [BEMIM] BF_4 and [BEMIM] PF_6 as a low cost and halide-free RTIL. This environmentally benign green method was found to be fast, simple and low temperature method which remarkably shortens preparation time and avoids the complicated synthetic procedures. The synthesized ion exchanged CdS was characterized by FT-IR, XRD, SEM, EDX and they were screened for their antimicrobial activities. From the antibacterial studies, it appeared that the all tested imidazolium ionic liquids stabilized CdS nanoparticles are the less effective products against the tested bacterial strains compared with the anti- microbial activity of pure ionic liquids except pure [BMIM] PF_6. The ionic liquids assisted nanoparticles can be directly used in various sensors, solar cell, fluorescence imaging of cancer cells and biological applications. Although the CdS structures formed are in nanosize for all the four ionic liquids, the lesser nanosize with discrete morphology was observed because of its longer alkyl group in its cation which is responsible for the obstruction of nanostructures from growing longer due to the steric hindrance effect.

Acknowledgements

The authors thank the Principal, and the Management of Sir Theagaraya College, Chennai -21 and Government Arts College, Thiruvannamalai for the constant encouragement and support rendered.

References

[1] C. A. Angell. ECS transactions. 3(7), 3 **(2010)**.

[2] C. Wang, L. Guo, H. Li, Y. Wang, J. Weng, L. Wu. *Green Chemistry*. 8, 603 **(2006)**.

[3] M. P. Reddy, A. Venugopal, M. Subrahmanyam. *Appl. Catal B*. 69, 164 **(2006)**.

[4] C. H. Wu, J. M. Chern. *Ind Eng Chem Res*. 45, 6450 **(2006)**.

[5] O. K. Dalrymple, D. H. Yeh, M. A. Trotz. *J Chem Technol Biotechnol*. 82, 121 **(2007)**.

[6] T. D. Dzhafarov, F. Ongul, S.A. Yuksel. *Vacuum*. 84(2), 310 **(2010)**.

[7] W. V. Huynh, J. J. Dittmer, A. P. Alivisatos. *Science*. 295(5564), 2425 **(2002)**.

[8] I. O. Oladeji, L. Chow, C. S. Ferekides, V. Viswanathan, Z. Zhao. *Sol. Energy Mater. Sol. Cells*. 61(2), 203 **(2000)**.

[9] L. E. Brus. *Appl. Phys. A: Mater. Sci. Process*. 53, 465 **(1991)**.

[10] S. Al-Bakri, K. S. Khashan, Z. A. Nima, E. A. Ajeel. *Advanced Materials and their application (SCNAMA)*. 13, 135 **(2009)**.

[11] K. Rajathi, A. Rajendran. *Inter. J. Engineer. Res. and General Sci*. 2(4), 252 **(2014)**.

[12] V. Taghvaei, A. Habibi-Yangjehand, M. Behboudnia. *J. Iran. Chem. Soc*. 7, 175 **(2010)**.

[13] N. Canillac, A. Mourey. *Food Microbiology*. 18, 261 **(2001)**.

[14] J. Zhu, Y. Shen, A. Xie, L. Qiu, Q. Zhang, S. Zhang. *J. Phy. Chem. C*. 111, 7629 **(2007)**.

[15] B. D. Cullity. Elements of X-Ray Diffraction. 2nd Ed: Addision Wesley, London **(1978)**.

[16] V. Singh, P. Chauhan. *J. Phys. Chem. Solids*. 70, 1074 **(2009)**.

[17] S. W. Cao, Y. J. Zhu, G. F. Cheng, Y. H. Huang. *J. Hazard Mater*. 171, 431 **(2009)**.

[18] K. S. Khashan, T. R. Marzoog, W. H. Mohammed, R. S. Noori. *Inter. J. Develop. Res*. 4(2), 211 **(2014)**.

This document was created with Win2PDF available at http://www.win2pdf.com.
The unregistered version of Win2PDF is for evaluation or non-commercial use only.
This page will not be added after purchasing Win2PDF.